ESTIMATION OF SITE AMPLIFICATIONS IN FOCAL AREA OF THE 2003 MIYAGIKEN-HOKUBU EARTHQUAKE USING AFTERSHOCK AND MICROTREMOR RECORDS

H. Yamanaka[1)], K. Motoki[2)], N. Komaba[3)], Y. Kamimura[3)] and M. Murayama[3)]

1) Associate Professor, Dept. of Environmental Sci. and Tech, Tokyo Institute of Technology, Japan
2)Assistant Professor, Dept. of built environments, Tokyo Institute of Technology, Japan
3) Graduate Student, Interdisciplinary Graduate School of Sci. and Tech., Tokyo Institute of Technology, Japan
yamanaka@depe.titech.ac.jp, kmoto@enveng.titech.ac.jp, komaban@depe.titech.ac.jp, kamimura@enveng.titech.ac.jp, mmrym@enveng.titech.ac.jp

Abstract: The 2003 Miyagiken-Hokubu earthquake (Mj=6.2) generated heavy damage in the northern part of Miyagi prefecture, Japan. Because of the shallow depth of the event, the damage was so limited in small area. In order to know ground motion characteristics and site effects in the focal area, we conducted observations of aftershocks and microtremors. The aftershocks were observed at 19 sites in 4 days just after the main shock on the 26th, July. We also conducted array observations of microtremors to know S-wave profiles down to the basement at 4 sites. The site amplification factors calculated form the deduced profiles agree with those estimated form the aftershock observations.

1. INTRODUCTION

Three major events (M5.5, M6.2, M5.3) occurred on the 26th, July, 2003, in the north of the Miyagi prefecture, Japan. Although these events are not so large as compared with the past destructive earthquakes, shallow depths of these events generated strong shaking in the focal area. Thus, sever damage was experienced in local cities in the focal area. In particular, some of old reinforced-concrete buildings and wooden houses were totally collapsed (e.g., Sato et al., 2003). Seismic intensities observed with seismic intensity meters in the focal area was 5-upper to 6 on the JMA scale during the main shock with Mj of 6.2. It is also reported that maximum accelerations at some sites were more than 1G. The maximum acceleration was 2.0G at the city office of Maruse-cho. However, strong ground motion records are not available at most of the seismic intensity stations. This also makes it difficult to understand relation between the damage and strong motion characteristics.

In this study, we conducted aftershock observations and microtremor array explorations in the focal area and the Ishinomaki plain to estimate strong motion characteristics with a focus on site effects.

2. GEOLOGICAL SETTING

Map of the studies area is shown in Fig. 1. Most of the area is covered with Quaternary soft soils. In the east of the area, pre-Tertiary granitic rock can be seen as an outcrop. We can see sedimentary layers in Tertiary age in the Asahiyama hill area that corresponds to the focal area of the main shock as

shown by broken lines in Fig.1. The thickness of the Quaternary layers over the Tertiary rock is estimated in the Ishinomaki plain in the east of the fault. It forms a basin structure whose maximum depth is about 80 meters at the center of the plain. The layers become shallower in the eastern and western sides of the plain. The depth to the pre-Tertiary basement in the plain is not well-known. However, we can qualitatively understand the basement depth distribution in the area from Bourguer anomaly map as shown in Fig.2. The positive gravity anomaly in the east of the area corresponds to outcrop of the pre-Tertiary basement.

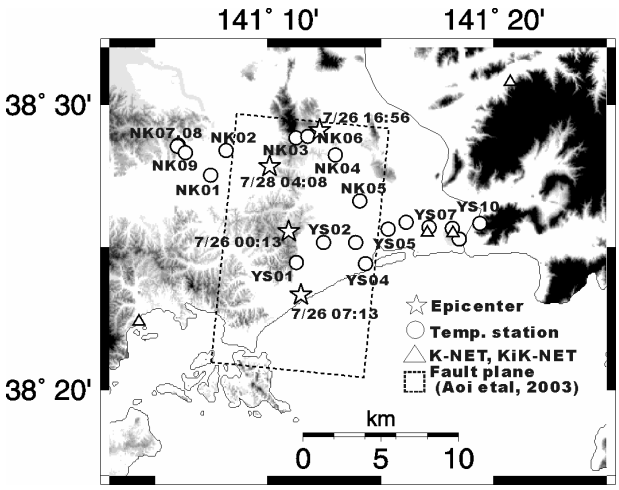

Fig.1 Map of studied area with aftershock observation stations.

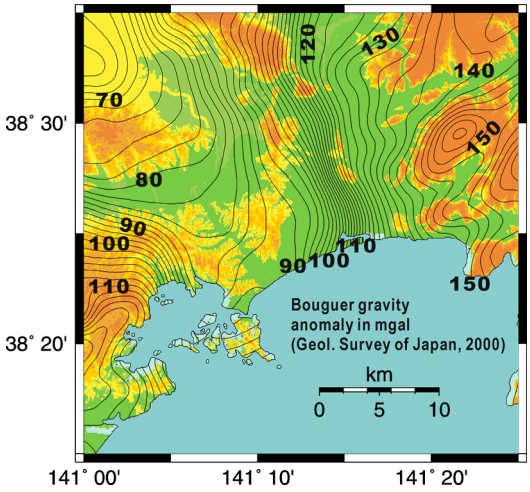

Fig.2 Bouguer gravity anomaly map

3. OBSERVATIONS OF AFTERSHOCKS AND MICROTREMORS

Aftershock observation was continued in four days starting on 27, September, 2003 at 19 stations which are indicated by circles in Fig.1.These stations are deployed with the following two viewpoints. The 10 stations from YS01 to YS10 were served to know nature of a layer phase seen in strong motion records at K-NET Ishinomaki station during the main shock. The station YS01 is situated at the foot of the Asahiyama hill covered with Tertiary layers. The stations of YS08 and 09 are also located on Tertiary layers, while pre-Tertiary basement can be seen near YS10. The other stations are on Quaternary layers in the Ishinomaki plain. The other objective is to estimate strong motion characteristics in the northern part of the focal area where the damage was so heavy. The stations from NK01 to NK09 were prepared for this purpose. It is noted that some of the stations were installed near the damaged buildings as explained later. A data recorder and a three-component accelerometer were installed at each station. Since we prepared 10 sets of the observational equipments, observational periods at some of the stations were only a half day. However, high activity of the aftershock sequences allows us to obtain enough number of seismic records to assess local site effects.

Observations of vertical microtremors in arrays were conducted at four sites in the area to explore subsurface S-wave profiles of the sediments over the pre-Tertiary basement. Most of the sites are located near the aftershock observation stations as shown in Fig.3. At each sites, two arrays were temporarily deployed in triangular or cross shape in different array sizes as shown in Fig.4. We observed vertical microtremors simultaneously at 7 stations in each array in 30 to 60 minutes.

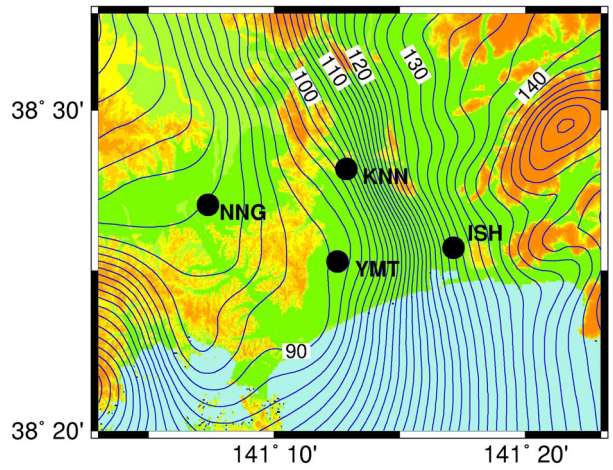

Fig.3 Locations of sites of microtremor array explorations

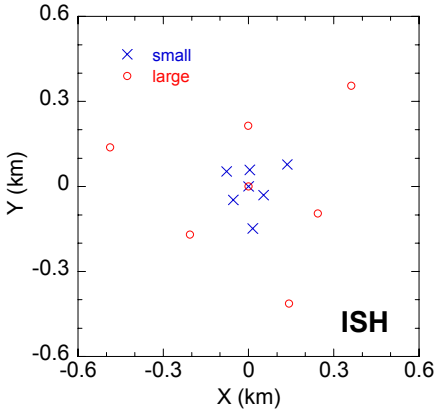

Fig.4 Example of microtremor arrays

4. ESTIMATION OF S-WAVE PROFILES

S-wave velocity profiles were deduced from analysis of the observed array data of vertical microtremors. Fig.5 shows the flow for data processing in the microtremor array exploration. Details can be seen in Yamanaka et al (2000). We, first, apply a frequency-wavenumber (f-k) spectral analysis (Capon, 1969). Then, a wavenumber vector for the maximum peak is found in f-k spectrum to estimate phase velocity at each period. These processes were repeated for all the segments of the array data. The final frequency-dependent phase velocity was obtained from averaging phase velocities for all the data in an array.

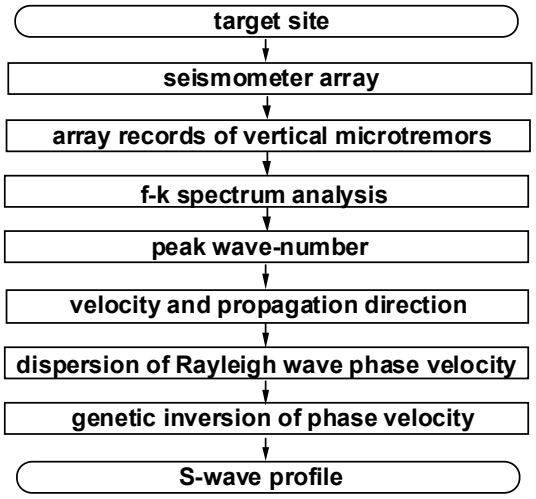

Fig.5 Flow for data processing in microtremor array exploration

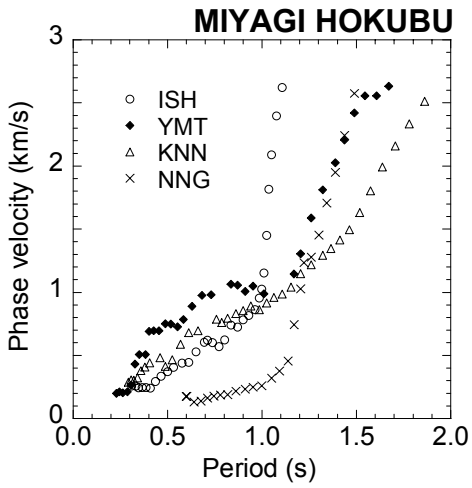

Fig.6 Phase velocity of vertical microtremors

The obtained phase velocities are shown in Fig.6. All the phase velocities clearly indicate dispersive features and can be regarded as that of Rayleigh waves. The phase velocity at ISH becomes rapidly large at periods of more than 1 second, indicating shallow depth to the basement. On the other hand, phase velocity at KNN is the lowest at periods of the more than 1.3 seconds. It is noted that the phase velocity at periods shorter than 1 second is extremely small at NNG, indicating the existence of low velocity layers near the surface.

We, next, invert the phase velocity at each site to a 1D S-wave velocity profile using an inversion technique. We apply a genetic inversion technique by Yamanaka and Ishida (1996). This method were successfully applied in many microtremor explorations in Japan (e.g., Yamanaka et al, 2000), because it does not require any specific initial model that must be usually prepared in least square methods. This method searches models with low misfit that is defined as L1-norm of differences between observed and synthetic phase velocities for fundamental Rayleigh wave. In the inversion, we assumed a 4-layers model and optimize S-wave velocity and thickness of each layer. Fig. 7 displays the inverted S-wave models. The depth basement with an S-wave velocity of 3.5 km/s is well correlated with the gravity anomaly map in Fig.2. The comparisons of the observed phase velocities with calculated ones for the inverted models are shown in Fig.8. The observed data can be well explained with inverted models.

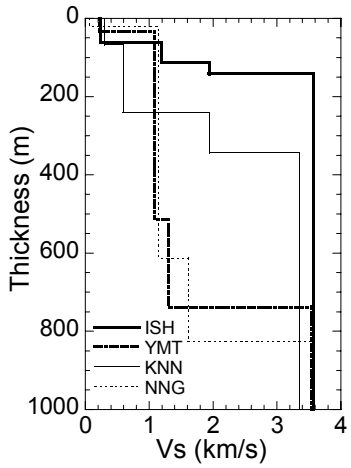

Fig.7 S-wave velocity profiles

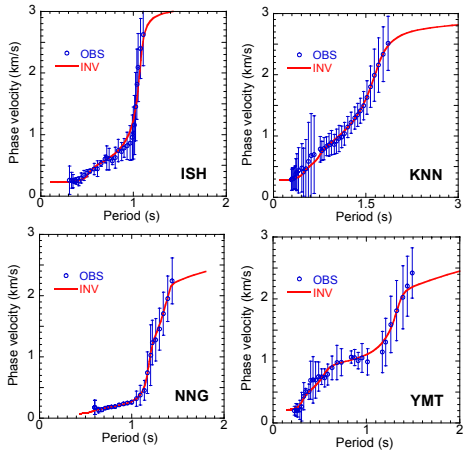

Fig.8 Comparison between observed and calculated phase velocities

5. ANALYSIS OF AFTERSHOCK RECORDS

5.1 Strong motion from large aftershock

In the aftershock observation, many events were recorded. However, most of them are small events with magnitudes of less than 2 and the maximum accelerations of less than 1 cm/s/s. The largest aftershock that we obtained is the event at 4:08 on 28th of July with an Mj of 5.0. The peak ground accelerations and velocities at YS01 to YS10 in our aftershock observations are shown in Fig.9 together with those from the K-NET. PGA and PGV calculated from the attenuation relations by Shi and Midorikawa (1999) are also shown in the figure. The observed PGAs for the aftershock are slightly larger than the calculated ones except for those in the focal area with a distance of less than 10 km. The observed PGVs are similar to those estimated from the attenuation equation for sites with surface S-wave velocities of 200 or 600 cm/s. These features of the PGA and PGV were also pointed out for the main shock (Motosaka, 2003). Therefore, it is indicated the PGV was normal to an event with similar size and only PGA in the focal area was extremely large. It is also noted that the PGVs in the Ishinomaki plain from our observations show a large variation by the differences of local geology. Such variation of the PGV must be appropriately incorporated in estimating strong motion in the area during the main shock.

North-south oriented ground velocities at YS01 to YS10 from the aftershock are displayed in Fig.10. The stations are almost situated in a line from the west to the east as can be seen in Fig.1. The development of the later phases is clearly identified in the stations in the Ishinomaki plain (YS02 to

YS07) indicating the strong effects of the sedimentary layers. In particular, the ground motion at YS07 is well dispersive and dominant at a period of 1 second. This later phase cannot be seen in the record at YS08 that is 1km apart in the east. Since YS08 is located on the hill with Tertiary layers, the later phases can be interpreted as effects of the Quaternary layers. In addition of the disappearance of the later phases, amplitude of the S-wave is much smaller at YS10 than that at YS08, because pre-Tertiary basement exists near the surface at YS10. These features can be also seen in the strong motion during the main shock. Fig. 11 shows the ground velocities during the main shock. The JMA and K-NET stations are located very close to YS08 and YS07 as shown in triangles in Fig.1, respectively. Since the ground motion features are very similar between the main shock and aftershocks, we can expect the existence of the later phases in Fig.10 during the main shock, too.

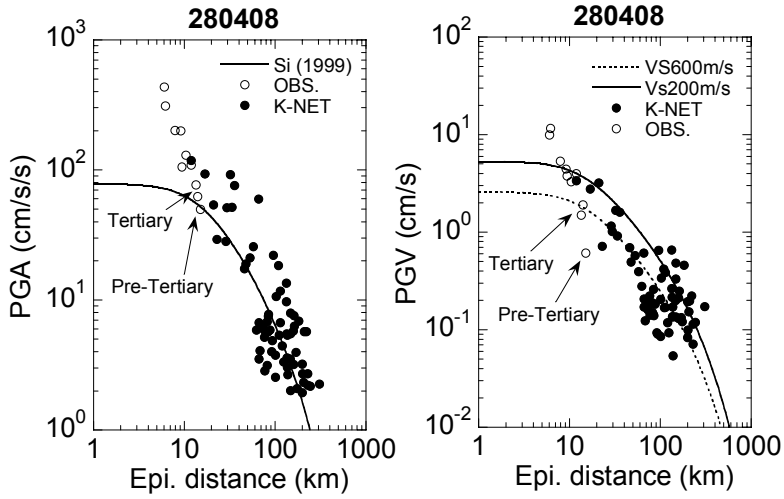

Fig. 9 Attenuations of PGA and PGV

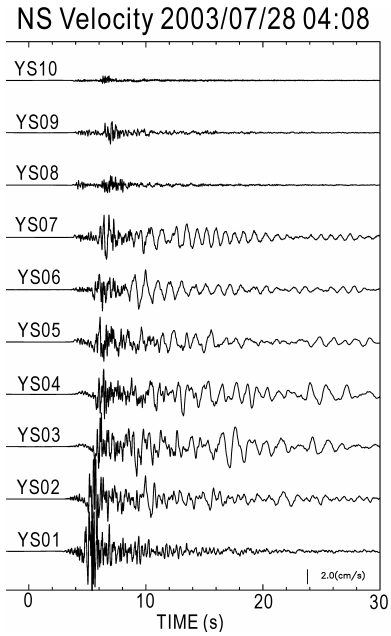

Fig.10 Observed ground velocity

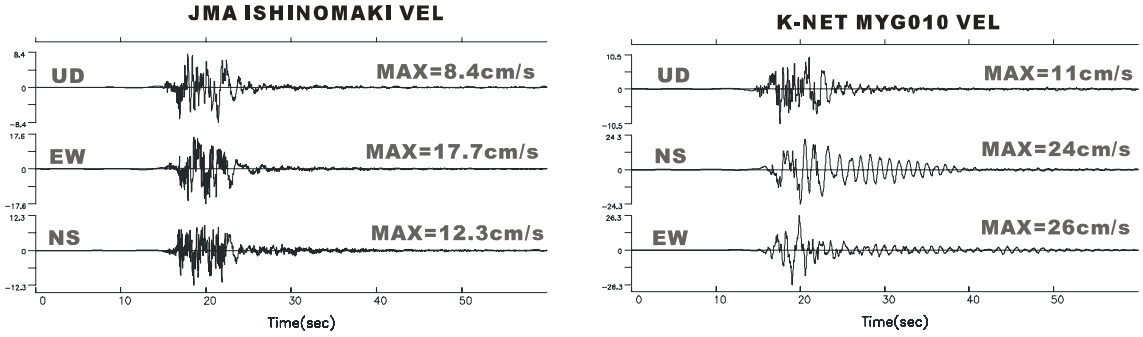

Fig.11 Strong ground motion during the main shock at JMA and K-NET

5.2 Spectral ratios at adjacent stations

As explained above, we installed our instruments at two adjacent stations with and without local soft soils. Fig. 12a shows the spectral ratios between YS07 and YS08. Two dominate peaks were found at periods pf 1.0 and 0.4 seconds in the ratio. In the figure, the ratio for the strong motions from the main shock is also shown by a broken line. Although the ratio are not completely the same, similar peak can be seen at a period of about 1 second. As explained above, the spectral ratio can be interpreted as amplification of S-wave in shallow Quaternary soft soils.

Next station pair is NK03 and NK06 in the Kanan-cho in the northern part of the focal area. NK06 is located in Kitamura Primary School where the most of columns at the first floor were heavily

damaged, while NK03 is 1 km apart from NK06 on the surface with no local soft soils. The spectral ratios of NK06 to NK03 in Fig.12b show amplification at periods of 0.1 to 0.3 seconds. Since this school is a three-story RC building, the amplification is one of the reasons for the heavy damage.

The last station pair consists of NK07 and NK08 in Kashimadai-cho. The distance between the two stations is just 100 meters as shown in Fig.13. NK07 is located close to 4-story RC building of Kashimadai Primary School that was moderately damaged. On the other hand, NK08 is located near the wooden school building. Although this wooden building is much older than the RC building, the wooden building has no damage at all. The spectral ratio between the two stations is shown in Fig.12c. The amplification is dominant at a period of 0.3 seconds. Probably this spectral ratio can be interpreted as amplification of artificial fills at NK07. Since the RC building stands between the filling and cutting parts of ground, this difference of site effects can be one of the reasons for its damage.

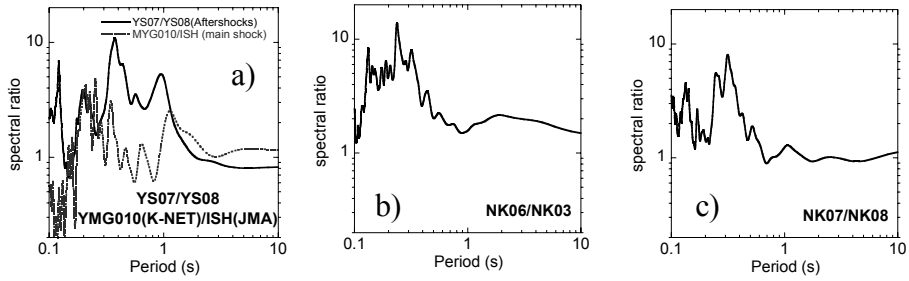

Fig.12 Spectral ratios at adjacent stations

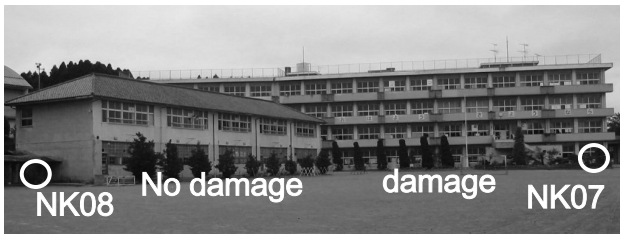

Fig.13 Locations of aftershock observation station of NK07 and NK08 in Kashimadai Primary School.

6. SITE AMPLIFICATIONS

The spectral ratio in Figs.12 suggests local site effects. However, they are regarded amplification of shallow Quaternary layers with low velocity. We can estimate site amplification for the shallow and deep sedimentary layers over the pre-Tertiary basement with an S-wave velocity of 3.5 km/s by taking the spectral ratio to records at YS10. Fig. 14 shows the spectral ratio of YS06 and 07 to that of YS10 for the aftershock discussed above. Although the spectral shape is similar to that in Fig.12a, absolute amplification is different from each other. This indicates that effects of deep sedimentary layers are necessary to estimate amplification factors. In the figure, theoretical amplification of S-wave in the S-wave profile deduced from the microtremor array exploration is also displayed. It agrees with the observed amplification.

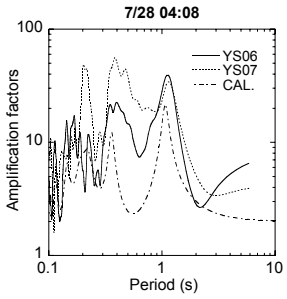

Fig.14 Ratio of spectra at YS06 and YS07 to that at YS10

There exist four layers in the S-wave profiles including the basement with an S-wave velocity of 3.5 km/s. We examine the effects of S-wave velocity of the bottom layer in calculation of theoretical amplification factors. The theoretical amplification factors are calculated with different S-wave velocity of the bottom layer in the models. Fig.15 shows the variation of the theoretical amplifications calculated for models at ISH from the microtremor array explorations. The thick solid line indicates the amplification of the model with a bottom layer velocity of 3.5 km/s. The amplification shown by the dotted line is calculated for the model where the 3rd layer is assumed as half space. Similarly, the amplification by thin line means the amplification for the model whose bottom layer has an S-wave velocity of 1.2 km/s. The comparisons of the amplifications clearly indicates that the importance of top Quaternary velocity layer in determining the amplification factors. We must pay special attention to model the Quaternary layer in strong motion calculation. Similar examination is conducted for the model at NNG shown in Fig.7. The spectral peak at 1 second can be modeled by considering the top Quaternary layers. However, amplification at periods of longer than 2 seconds can not be explained with consideration of only the top two layers. Therefore, deep sedimentary layers over the basement must be incorporated in synthetics of long-period motions in the area.

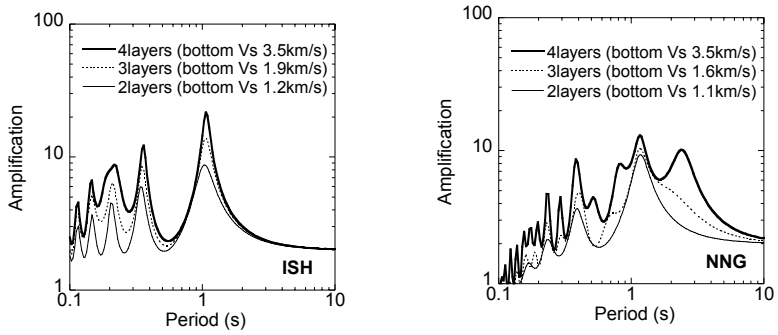

Fig.15 Variation of amplification factors with different S-wave velocity for the bottom layers in computational models at ISH (left) and NNG (right)

7. CONCLUSIONS

We conducted observation of aftershocks of the 2003 Miyagiken-Hokubu earthquake in Miyagi prefecture, Japan, to estimate local site effects. Strong motion instruments were temporarily deployed at 19 stations in the focal area of the main shock. We also conducted microtremor array observations at four sites in the area to know S-wave velocity profiles over the basement. The four-layer models for shallow and deep sediments are deduced from the microtremor array explorations. We estimate site amplification from spectral ratios of observed records from aftershocks. The amplification estimated is in agreement with the calculated one from the S-wave profiles deduced in the microtremor explorations.

Acknowledgements:

We thank people to allow us observation of aftershocks and microtremors. The strong motion data used in this study are provided by the K-NET and KiK-net of the National Research Institute for Earth Science and Disaster Prevention, and by Japan Meteorological Agency. This study supported by Grant-in-Aid for General Scientific Research (#15800009) from Japan Ministry of Education, Culture, Sport, Science, and Technology, Japan.

References:

Capon, J.(1969), "High resolution frequency wavenumber spectrum analysis", *Proc. IEEE*, 57, pp1408-1418.

Motosaka, M. (2003), "Report of damage of July 26, 2003 Miyagiken-hokubu earthquake –earthquake and ground

motion-," Earthquake Disaster Prevention, 193, 41-46 (in Japanese).
Sato, T., S. Phno, and M. Motosaka (2003), "A quick report of seismic disaster for the Earthquake (July 26, 2003) occurred on norhern part of Miyagi prefecture, J. of Japan Soc. For Natural Disaster Science,22,149-157 (in Japanese).
Si H. and S. Midorikawa, S. (1999), "New attenuation relationships for peak ground acceleration and velocity considering effects of fault type and site conditions," *J. Struct. Constr. Eng.,* Arch. Inst. Jap*.,* 523, 63-70 (in Japanese).
Yamanaka,H. N. Yamada,H. Sato, S. Oikawa, Y. Ogata, K. Kurita, K. Seo, and Y.Kinugasa (2000) "Exploration of basin structure by microtremor array technique for estimation of long-period ground motion," *The 12th World Conf. Earthq. Eng., CDROM* No.1484.
Yamanaka, H. and H. Ishida (1996) Application of genetic algorithms to an inversion of surface-wave dispersion data, *Bull. Seism. Soc. Am*. Vol.86, No.2, 436-444.